Erschienen in: IEEE Journal of Photovoltaics ; 7 (2017), 6. - S. 1627-1634
https://dx.doi.org/10.1109/JPHOTOV.2017.2755072

Degradation of Surface Passivation on Crystalline Silicon and Its Impact on Light-Induced Degradation Experiments

David Sperber, Alexander Graf, Daniel Skorka, Axel Herguth, and Giso Hahn

***Abstract*—A decrease of surface passivation quality is observed in FZ, Cz, and mc-Si lifetime samples during light-induced degradation (LID) treatments. It is shown that this degradation occurs not only in samples with single SiN_x:H layers but also when using layer stacks consisting of SiO_x/SiN_x:H or AlO_x:H/SiN_x:H. Time-resolved calculation of the surface saturation current density J_{0s} is shown to be a reliable method to separate changes in the bulk and at the surface of samples during LID treatments. The impact of the observed changes in passivation quality on the outcome and interpretation of LID experiments aiming at changes in the bulk of Cz or mc-Si is investigated and discussed.**

***Index Terms*—Aluminum oxide, charge carrier lifetime, crystalline silicon, degradation, float-zone, silicon nitride, silicon oxide, silicon photovoltaics, stability, surface passivation.**

I. Introduction

LIGHT-INDUCED degradation (LID) [1] such as boron–oxygen (BO) related degradation in Czochralski silicon (Cz-Si) [2]–[4] or LID in multicrystalline silicon (mc-Si) [5]–[7] can severely reduce bulk minority charge carrier lifetime τ_b in crystalline silicon and thereby limit the efficiency of solar cells, especially if the concept relies on high τ_b like a passivated emitter and rear cell (PERC) concept [8]. However, both types of LID can be followed by subsequent regeneration of τ_b [9]–[12] allowing for permanent curing of LID in the bulk. Once τ_b is sufficiently high, surface passivation becomes the limiting factor and renders solar cells more susceptible to degradation of surface passivation.

In LID experiments on lifetime samples, it has already been shown that, indeed, passivation quality of SiN_x:H layers or stacks thereof changes in the course of time [13]–[15]. However, interpretation of measurement data can be quite tricky as bulk and surface-related recombination (and changes thereof) both determine the measured effective lifetime τ_{eff}.

In this study, we investigate changes in surface passivation during LID treatments of lifetime samples made of different Si materials. First, it will be shown that a time- and injection-resolved visualization of lifetime data and a time-resolved calculation of the surface saturation current density J_{0s} [16] are useful tools for assessing the degree of degradation in surface passivation, even in the case of changes of τ_b during an ongoing treatment. This method is then applied to compare different passivation layers with regard to severity and timescale of surface-related degradation. Subsequently, a Cz-Si and a mc-Si sample are presented to investigate the impact of changes in surface passivation quality on long-term LID experiments aimed at observing changes in the silicon bulk. Finally, possible surface-related degradation mechanisms are discussed.

II. Experimental

A. Sample Preparation

Samples were made of either B-doped float-zone silicon (FZ-Si), Cz-Si, or mc-Si, or P-doped FZ-Si. Because a wide variety of processing parameters was used, standard processing is described here and deviations of this process as well as sample thickness are described in the figure captions.

For most samples, material with a specific resistivity $\rho \approx 2\ \Omega{\cdot}\mathrm{cm}$ was used. Cz-Si, mc-Si, and selected FZ-Si samples first received a saw damage etch in KOH at 80 °C, followed by a chemical polish (CP) etch in a solution of nitric acid, acetic acid, and hydrofluoric acid (HF) at room temperature. All but selected FZ-Si samples were then wet-chemically oxidized in a solution of H_2O_2 and H_2SO_4 at 80 °C, followed by a dip in HF to remove impurities from the sample surface (Piranha clean).

Samples with single SiN_x:H layers were coated on both sides in an industrial direct plasma-enhanced chemical vapor deposition (PECVD) with a frequency of 40 kHz. Samples with a SiO_x/SiN_x:H stack first received ∼10 nm SiO_x in a thermal oxidation at 900 °C before deposition of SiN_x:H in a laboratory direct plasma PECVD at 13.56 MHz. Samples passivated with AlO_x:H/SiN_x:H received ∼10 nm of atomic layer deposited AlO_x:H (refractive index $n \approx 1.7$ at 600 nm) followed by SiN_x:H deposition in an industrial remote plasma PECVD at 2.45 GHz. All SiN_x:H layers had a thickness of ∼75 nm and $n \approx 2.0$ at 600 nm.

Afterwards, samples were fired in a fast firing belt furnace. Temperature profiles were tracked on selected samples with a thin type K thermocouple contacting the upper side of a sample by mechanical prestrain, thereby not changing sample properties significantly. The mc-Si sample was fired at a measured peak

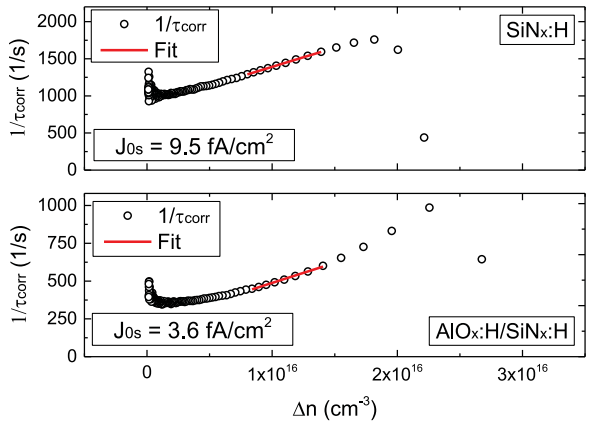

Fig. 1. (Top) Inverse corrected lifetime data $1/\tau_{\rm corr}$ and J_{0s} fit of a B-doped FZ-Si sample ($\sim$1 Ω·cm, 250 μm) passivated with SiN_x:H. (Bottom) $1/\tau_{\rm corr}$ and J_{0s} fit of a B-doped FZ-Si sample ($\sim$2 Ω·cm, $\sim$180 μm) passivated with AlO_x:H/SiN_x:H. Measurements were taken before LID treatments started.

sample temperature of $\sim$730 °C. AlO_x:H/SiN_x:H passivated samples were fired at $\sim$750 °C. All other samples were fired at $\sim$800 °C. After firing, samples were stored in darkness at room temperature until LID treatments started.

B. LID Treatments and Measurement Techniques

Samples were treated at $\sim$1 sun equivalent illumination intensity at elevated temperatures ranging from 80 °C to 150 °C. Illumination was achieved with halogen incandescent lamps and illumination intensity was measured using a solar cell. One sun equivalent illumination was achieved by matching the short-circuit current $j_{\rm sc}$ of the measurement cell under the treatment illumination to that under a solar spectrum simulator (see [17] for further discussion of the unit "sun equivalent").

To measure $\tau_{\rm eff}$, samples were repeatedly taken from a treatment hotplate, and a photoconductance decay (PCD) measurement was carried out at 30 °C using the generalized mode of a Sinton Instruments lifetime tester (WCT-120). In most graphs, $\tau_{\rm eff}$ is shown at an injection $\Delta n \approx 0.1\,N_d$, with N_d being the doping density. Injection-resolved graphs, on the other hand, feature a color-coded range of $\tau_{\rm eff}$ at different Δn.

To quantify recombination at the surface, we apply the approach for determination of the emitter saturation current density J_{0e} as described by Kimmerle *et al.* [18]: First, inverse corrected lifetime data $1/\tau_{\rm corr}$ are calculated which take into account bandgap narrowing [19], [20], a potential Shockley–Read–Hall recombination in the bulk [21], [22], and a diffusion correction which may be necessary at higher injection. We use this approach on samples without emitter, and a linear fit of $1/\tau_{\rm corr}$, therefore, yields the surface saturation current density J_{0s} [16] as shown in two examples in Fig. 1.

The range of Δn for the fit of J_{0s} is set from $8\cdot10^{15}$ to $1.5\cdot10^{16}$ cm^{-3} with the exception of one 200 Ω·cm sample where Δn ranges from $5\cdot10^{15}$ to $8\cdot10^{15}$ cm^{-3} due to a limited injection range of PCD measurement data. The upper limit makes sure that measurement artifacts at the beginning of a PCD measurement (equaling highest Δn) do not influence the J_{0s} fit while the overall restriction to measurement data to rather high Δn further reduces influences of changes in τ_b on the determination of J_{0s}.

While the linear fit is of good quality in most cases (Fig. 1, top), samples with very low $J_{0s} < 5$ fA/cm^2 show a slight bow in $1/\tau_{\rm corr}$ data used for the fit of J_{0s} (Fig. 1, bottom). Comparing different fit ranges between $\Delta n = 5\cdot10^{15}$ and $1.5\cdot10^{16}$ cm^{-3} results in an estimated uncertainty of the absolute value of J_{0s} of $\sim$20%, increasing up to $\sim$50% when $J_{0s} < 5$ fA/cm^2. However, as will be shown later, relative changes of J_{0s} during sample treatment exceed this uncertainty by far, making relative changes in J_{0s} well visible.

Time-resolved photoluminescence imaging (TR-PLI) [23], [24] was used for mc-Si samples instead of PCD. This offers the advantage of self-calibrated spatially resolved measurement data of $\tau_{\rm eff}$, however, without covering the broad range of Δn values of a PCD measurement.

C. Superacid Repassivation of Sample Surfaces

Dielectric passivation layers were removed from some samples after LID treatment, and samples were repassivated to gain further information about the cause of degradation.

The removal of dielectrics was accomplished by immersing samples in $\sim$10% HF. Afterwards, samples received a CP etch for 2 min, removing $\sim$1 μm per side. This was followed by a Piranha clean as described before. Directly before repassivation, samples were again etched in 25% tetramethylammonium hydroxide for 10 min at $\sim$80 °C to remove $\sim$5 μm on each side. In the next step, samples were dipped in 1% HF before they received a clean in a solution of H_2O, H_2O_2, and HCl for 10 min at $\sim$75 °C. After another dip in 2% HF, samples were immersed in a nonaqueous solution of bis(trifluoromethane)sulfonimide dissolved in dichloroethane (2 mg/ml) for $\sim$60 s. This procedure leads to very good passivation of sample surfaces as described in [25] and [26] while only subjecting a sample to moderate temperatures, therefore leaving its defect properties rather unchanged. Calculating values of J_{0s} after repassivation as described in the previous section results in values $\sim$2 fA/cm^2 on a P-doped sample and values ranging from 5 to 12 fA/cm^2 on B-doped samples in this study.

III. Results

A. Changes in B-Doped FZ Samples Passivated With SiN_x:H

Part of the data discussed in this section have already been presented in [15] and [27]. They are shown again to assess the quality of J_{0s} values and to introduce methods that will be used on other samples in subsequent sections.

Already at 80 °C and $\sim$1 sun equivalent illumination, a B-doped FZ-Si sample passivated with SiN_x:H shows strong changes in $\tau_{\rm eff}$ (Fig. 2, black data). Because FZ-Si is lean in impurities and oxygen, one could easily assume that all of these changes occur due to changes in passivation quality. However, a closer examination using corona charging series (CC, green data) and capacitance voltage measurements (blue data) on identically processed samples reveals that neither chemical passivation quality nor fixed charge density Q_f change significantly in the short term (<10 h). A closer investigation in [15] and [28], including repassivation of sample surfaces, leads to the

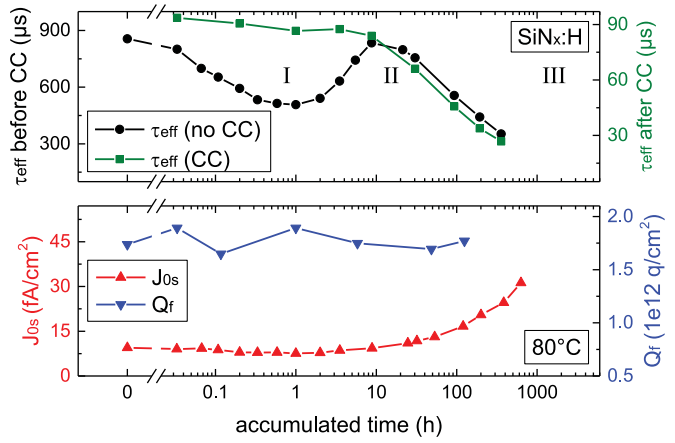

Fig. 2. (Top) PCD measurement of τ_{eff} before and after depositing corona charges (CC) on a sample treated at 80 °C and ∼1 sun equivalent illumination. The B-doped FZ-Si sample (∼1 Ω·cm, 250 μm) was passivated with SiN_x:H. (Bottom) Evaluation of J_{0s} and Q_f of two other identically processed and treated samples. All data except J_{0s} values are taken from [15].

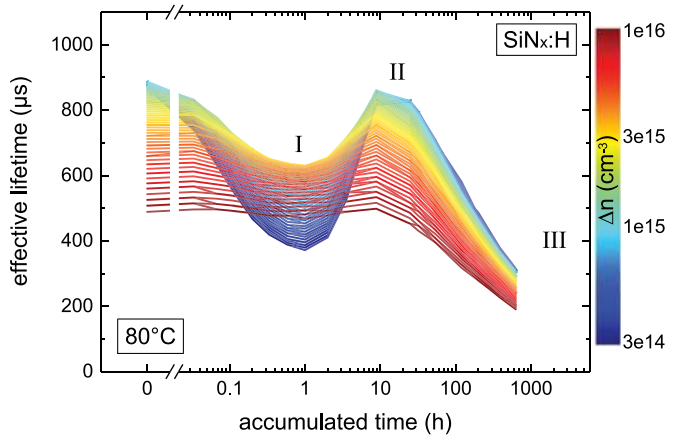

Fig. 3. Injection-resolved evolution of τ_{eff} during LID treatment at 80 °C and ∼1 sun equivalent illumination of the B-doped FZ-Si sample used for the determination of J_{0s} in Fig. 2. Injection levels are color-coded, ranging from $\Delta n = 3{\cdot}10^{14}$ cm^{-3} (blue) to $\Delta n = 1{\cdot}10^{16}$ cm^{-3} (red). Data taken from [27].

conclusion that the first minimum and maximum in τ_{eff} (denoted with roman numbers I and II in Fig. 2) are actually caused by a degradation and regeneration of τ_b.

For longer treatment times (>10 h), the renewed decrease of τ_{eff} is, however, surface related: the chemical passivation quality of the sample decreases as can be seen in the CC state of the sample with minimum field effect passivation (green data, note the different scaling), leading to a significant decrease in τ_{eff} as well. This decrease of surface passivation quality has been verified by wet-chemical repassivation of the sample surface in [15] and is correlated with increasing J_{0s} values (Fig. 2, red data). As can be seen, J_{0s} reflects changes at the surface pretty well and changes only little during changes of τ_b in the first hours of treatment. The changes in the bulk and at the surface are also revealed in an injection-dependent visualization of lifetime data as introduced in [25] and shown in Fig. 3. Here, it can be clearly seen that degradation and regeneration (I) of τ_b are especially

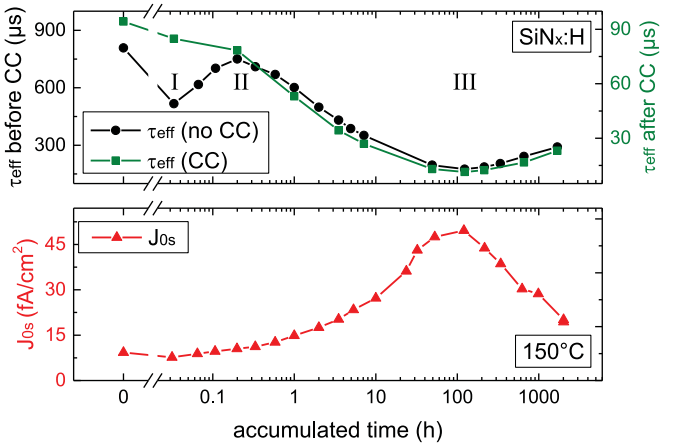

Fig. 4. (Top) Measurement of τ_{eff} before and after depositing corona charges on a B-doped FZ-Si sample treated at 150 °C and ∼1 sun equivalent illumination. The sample was processed in the same way as the ones shown in Fig. 2. (Bottom) Evaluation of J_{0s} of an identically processed and treated sample. All data except J_{0s} values are taken from [15].

pronounced at low injection (blue data) as would be expected from a deep level defect. The degradation of surface passivation (III), on the other hand, shows an inverted injection dependence with lifetime values decreasing over the whole injection range. This is in good agreement with the increasing J_{0s} values shown in Fig. 2 which arise due to a stronger limitation of τ_{eff} with increasing Δn.

Increasing the treatment temperature to 150 °C leads to an accelerated sample evolution as can be seen in Fig. 4. The degradation of chemical passivation quality reaches a minimum III after ∼100 h of treatment time, and afterwards a recovery of chemical passivation quality sets in. At 250 °C, τ_{eff} even recovers to values higher than the initial τ_{eff} [15].

B. *Degradation of SiO_x/SiN_x:H Passivation Layers*

So far, samples were passivated with SiN_x:H only which leads to the question whether the surface-related degradation can be avoided by using other passivation layers. Fig. 5 shows a B-doped FZ-Si sample (∼2 Ω·cm) passivated with a SiO_x/SiN_x:H stack. Already after short illumination, a strong increase in τ_{eff} can be observed. Additionally, J_{0s} does not change significantly in the first minutes of treatment and a crossover in injection-resolved measurement data can be observed at $\Delta n \approx 1{\cdot}10^{14}$ cm^{-3} (data not shown). Therefore, it is assumed that this sample suffers to some degree from iron contamination, resulting in FeB dissociation and increased τ_{eff} after short illumination [29]. For longer treatment times, however, a strong degradation of τ_{eff} can be seen and the increasing J_{0s} indicates that this degradation is related to the surface of the sample, similar to the SiN_x:H samples discussed before. Wet chemical repassivation of the sample after treatment confirms this finding: τ_{eff} increases from ∼140 μs to ∼1.5 ms ($\Delta n \approx 0.1$ N_d), proving that τ_b is still very high.

The injection-resolved visualization of measurement data shown in Fig. 6 additionally reveals that this sample suffers from a slight degradation at low injection (blue) during the first hours of treatment, leading to the shoulder in Fig. 5 at around ∼10 h.

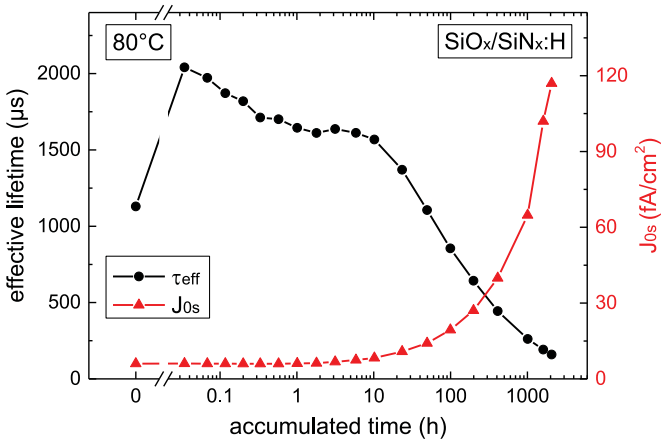

Fig. 5. Measurement of τ_{eff} (black) and J_{0s} (red) of a B-doped FZ-Si sample ($\sim$2 Ω·cm, 250 μm) passivated with SiO_x/SiN_x:H and treated at 80 °C and $\sim$1 sun equivalent illumination. Instead of wet-chemical cleaning, the sample received only a dip in HF before thermal oxidation.

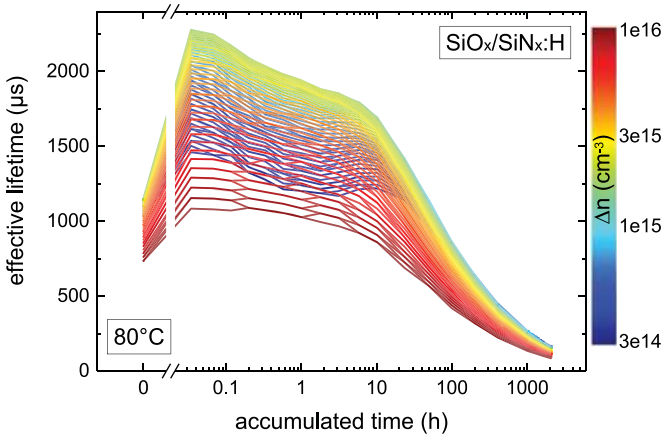

Fig. 6. Injection-resolved evolution of τ_{eff} of the B-doped FZ-Si sample shown in Fig. 5.

This is probably related to the bulk degradation described in Section III-A. It is noteworthy that FZ-Si bulk degradation appears to be much weaker in a SiO_x/SiN_x:H passivated sample compared to a SiN_x:H passivated sample. However, the bulk degradation is not the scope of the current study and ongoing experiments aim at clarifying where the difference in bulk degradation originates from.

As was already observed in [27], degradation in surface passivation quality also affects P-doped samples with SiN_x:H passivation. To compare the surface-related degradation of SiO_x/SiN_x:H passivated samples made of different base materials, their J_{0s} values are shown in Fig. 7. While all samples are affected by degradation in surface passivation quality, it seems that the degradation progresses slower or less pronounced on the lightly B-doped and P-doped samples. Wet chemical repassivation of the P-doped sample after treatment leads to an increase from $\sim$810 μs to $\sim$4.5 ms, confirming a significant surface-related degradation.

Additionally, a recovery of surface passivation quality has been observed in SiO_x/SiN_x:H passivated samples at higher

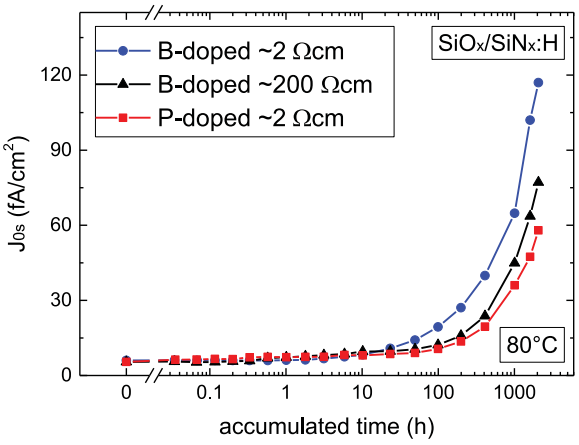

Fig. 7. Evolution of J_{0s} of samples made of different FZ-Si base material and treated at 80 °C and $\sim$1 sun equivalent illumination. All samples (thickness 250 μm) were processed identically and passivated with SiO_x/SiN_x:H. Instead of wet-chemical cleaning, the samples received only a dip in HF before thermal oxidation.

treatment temperatures, similar to the SiN_x:H sample shown in Fig. 4 (data not shown).

C. *Degradation of AlO_x:H/SiN_x:H Passivation Layers*

Passivating a B-doped FZ-Si sample with AlO_x:H/SiN_x:H may lead to a surface-related degradation, too, as can be seen in Figs. 8 and 9. The sample first underwent an LID treatment at 150 °C and $\sim$1 sun equivalent illumination for 12 min because it served as a reference for BO-regenerated Cz-Si samples. It was then treated at 80 °C and $\sim$1 sun equivalent illumination. The sample first shows a slight degradation and regeneration of τ_{eff} during the first hours of treatment. These changes are most pronounced at low injection (Fig. 9, blue data) and probably related to changes in the FZ-Si bulk as already described before. It seems likely that the initial treatment at 150 °C was too short to fully regenerate the FZ-Si bulk and therefore, some degradation and regeneration still occur after the initial LID treatment at higher temperature.

After treatment times >100 h, surface-related degradation sets in according to rising J_{0s} values. Wet chemical repassivation after LID treatment leads to an increase of τ_{eff} from $\sim$0.9 to $\sim$1.1 ms ($\Delta n \approx 0.1$ N_d). The J_{0s} value after repassivation was, however, comparably high ($\sim$12 versus $\sim$5 fA/cm^2 in other repassivated samples) and therefore only slightly lower compared to the already degraded J_{0s} value of the sample before repassivation ($\sim$15 fA/cm^2). This explains the rather low difference between the value before and after repassivation.

Compared to SiN_x:H and SiO_x/SiN_x:H samples, the degradation occurs at a later point in time. Similarly processed AlO_x:H/SiN_x:H passivated Cz-Si samples degrade on a similar timescale but less strongly compared to the FZ-Si sample (data not shown). It might be possible that the FZ-Si sample shown in Fig. 8 received an atypical dielectric deposition (optically inhomogeneous sample surface) and therefore suffers from stronger degradation. However, it can be stated that even an AlO_x:H/SiN_x:H passivated sample may degrade significantly. Similar to the samples discussed before, a recovery of passi-

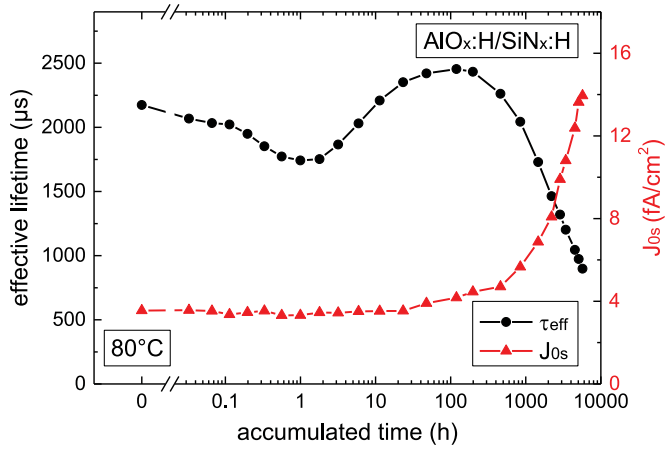

Fig. 8. Measurement of τ_{eff} (black) and J_{0s} (red) of a B-doped FZ-Si sample ($\sim$2 Ω·cm) passivated with AlO_x:H/SiN_x:H. The sample was etched to $\sim$180 μm before sample processing. The sample underwent LID treatment at 150 °C and $\sim$1 sun equivalent illumination for 12 min before being treated at 80 °C and $\sim$1 sun illumination.

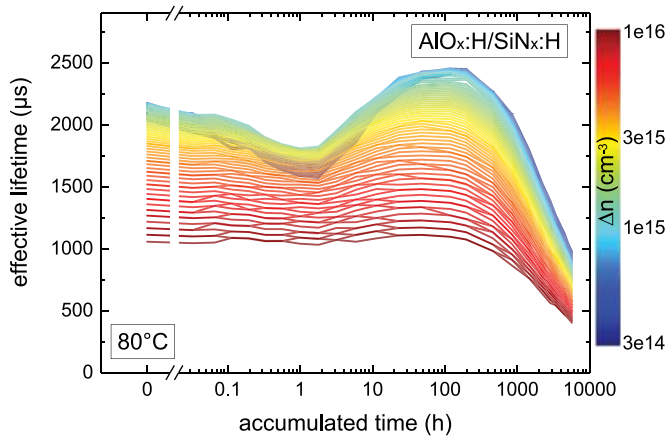

Fig. 9. Injection-resolved evolution of τ_{eff} of the B-doped FZ-Si sample shown in Fig. 8.

vation quality has been observed in AlO_x:H/SiN_x:H passivated samples at higher treatment temperatures (data not shown).

D. Impact on LID Experiments in Cz-Si and mc-Si

With respect to the pronounced changes in passivation quality of FZ-Si samples, the question naturally arises whether the observed surface degradation also affects other Si materials. Fig. 10 illustrates results from both a B-doped mc-Si and Cz-Si sample passivated with SiN_x:H. The Cz-Si sample was already treated at 150 °C and $\sim$1 sun equivalent illumination for 12 min to regenerate BO-related defects before the treatment shown in Fig. 10 started. Therefore, the sample shows negligible degradation and regeneration of τ_b due to BO-related defects during the first hours of treatment (black data). For long treatment times, a strong decrease of τ_{eff} is observed. This decline could easily be interpreted as instability of the regenerated state of the BO-related defect. However, the decline occurs on the same timescale as the surface degradation observed in FZ-Si samples

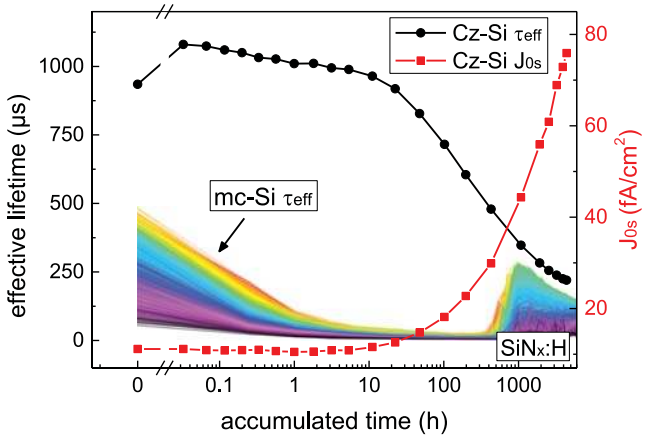

Fig. 10. *Single curves:* τ_{eff} at $\Delta n = 2.1\cdot10^{15}$ cm^{-3} (black) and J_{0s} (red) of an already BO-regenerated Cz-Si sample (B-doped, $\sim$2 Ω·cm, $\sim$180 μm) passivated with SiN_x:H during LID treatment at 80 °C and $\sim$1 sun equivalent. *Color array:* Spatially resolved degradation and regeneration of a B-doped mc-Si sample ($\sim$1 Ω·cm, 180 μm) treated at 75 °C and $\sim$1 sun equivalent. Shown are τ_{eff} data from different spots of the sample surface taken with TR-PLI. The data were color coded depending on the initial τ_{eff} value, ranging from low (black) to high lifetimes (red). Part of the data is taken from [12]. The injection of the mc-Si sample was estimated to be $\Delta n \approx 2.1\cdot10^{15}$ cm^{-3} at 250 μs. Therefore, the Cz-Si data are also shown at this Δn.

and additionally features the same increase of J_{0s} (red data). Wet chemical repassivation of the sample surface after LID treatment leads to an increase in τ_{eff} from $\sim$250 μs to $\sim$1.5 ms at $\Delta n \approx 0.1\ N_d$, verifying that the decrease of τ_{eff} is caused by surface-related degradation and that τ_b remains very high even after $\sim$4400 h of treatment at 80 °C and $\sim$1 sun equivalent illumination.

Fig. 10 also shows τ_{eff} data of TR-PLI measurements of a mc-Si sample treated at 75 °C and $\sim$1 sun equivalent illumination. Each line represents a different spot on the sample surface and lines are color-coded according to the initial τ_{eff} value of each spot as further discussed in [12]. In the first $\sim$300 h, τ_{eff} decreases strongly due to LID in the mc-Si bulk. However, when regeneration sets in after $\sim$300 h of treatment time, it can be seen that τ_{eff} does not reach values comparable to the initial values anymore, and after $\sim$1000 h, starts to degrade again.

Comparing the mc-Si τ_{eff} data to the τ_{eff} values of the regenerated Cz-Si sample for times >1000 h reveals that this behavior can be explained with a degradation of surface passivation quality: when regeneration of the mc-Si sample sets in, the surface passivation has already degraded significantly and, therefore, even a sample with fully regenerated τ_b cannot achieve the same τ_{eff} compared to the initial value before treatment. Wet chemical repassivation of similarly processed mc-Si samples confirms this long-term degradation of surface passivation quality in mc-Si samples and will be discussed in a separate publication.

IV. Discussion

For all samples shown, time-dependent J_{0s} values were calculated according to the method for the calculation of J_{0e} described by Kimmerle *et al.* [18]. Absolute values of J_{0s} may suffer from some uncertainty when J_{0s} is very low due to a slight bow in corrected inverse lifetime data. However, it appears that J_{0s} val-

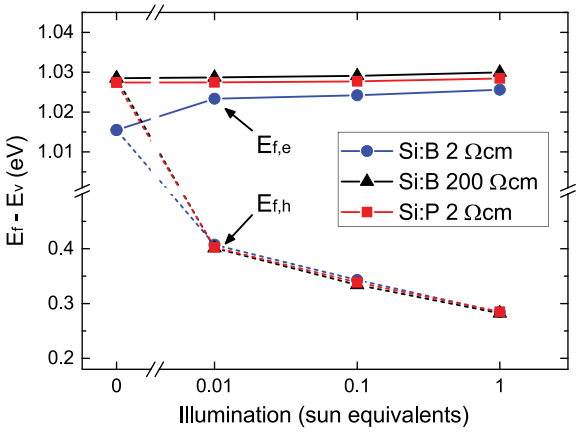

Fig. 11. Simulation of quasi-Fermi levels at the silicon surface at different illumination conditions. Values are given relative to the valence band edge.

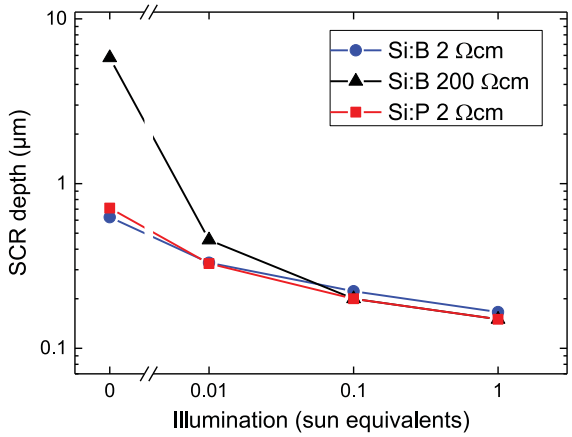

Fig. 12. Simulation of the depth of the space charge region at different illumination conditions.

ues reflect relative changes in surface passivation quality with good accuracy while only changing slightly during changes of τ_b. This makes the calculation of J_{0s} a promising approach for the separation of changes in the bulk and at the surface in LID studies on lifetime samples.

A strong degradation of surface passivation quality was observed in samples passivated with either SiN_x:H or SiO_x/SiN_x:H after prolonged treatment. The comparison of differently doped base material passivated with SiO_x/SiN_x:H revealed differences: A more heavily B-doped sample appears to degrade faster/more pronounced compared to a lightly B-doped or a P-doped sample.

To gain a better understanding of possible degradation mechanisms, samples with different base material but identical surface passivation were simulated using PC1Dmod 6.2.1 [30]. For this purpose, a surface recombination velocity $S_n = S_p =$ 250 cm/s and a fixed charge density of $Q_f = +5{\cdot}10^{11}$ q cm^{-2} were assumed for all samples. These values correspond to $J_{0s} \sim$ 5fA/cm^2 in the P-doped sample, according to [16], which closely resembles the initial value in Fig. 7.

The positive fixed charge density enforces an n-type inversion layer at the surface of p-type substrates while it results in an n-type accumulation layer in n-type substrates. Therefore, the position of Quasi Fermi levels $E_{f,i}$ at the silicon surface is mostly defined by the amount of fixed charge in the dielectric and does not change significantly when using a different base material as can be seen in Fig. 11. Hence, the carrier concentrations close to the surface are also similar, especially under illumination: At 1 sun equivalent, charge carrier concentrations do not differ by more than 12% rel. in the simulated samples. According to Fig. 12, the depth of the space charge region is also very similar at stronger illumination. Therefore, a difference in degradation behavior of samples made of different base materials seems to be neither related to different carrier concentrations nor position of $E_{f,i}$ at the silicon surface. Still, the real samples could differ in other parameters besides base doping. Since only three samples with different base material have been investigated here, more experiments are necessary to verify if the observed degradation in surface quality is linked to the substrate doping.

A similar but much slower surface-related degradation was observed in samples passivated with AlO_x:H/SiN_x:H. Niewelt *et al.* have reported on samples which show only a slight degradation of this passivation layer stack under similar treatment conditions [31]. This shows that AlO_x:H/SiN_x:H passivated samples can be, in principle, rather stable. The results shown in Fig. 8, on the other hand, indicate that also AlO_x:H/SiN_x:H may suffer from a significant degradation of surface passivation quality, even at 80 °C. At 150 °C, AlO_x:H/SiN_x:H samples degrade much faster as was observed in [13]. So far, it remains unclear where the difference between rather stable and rather unstable AlO_x:H/SiN_x:H samples arises from and future research is aimed at clarifying this issue.

However, even the AlO_x:H/SiN_x:H sample shown in Fig. 8 degrades much slower compared to SiN_x:H passivated samples and it can be concluded that an AlO_x:H interlayer, while not preventing it entirely, slows down the surface-related degradation significantly. This could be related to a different band structure close to the sample surface: While SiN_x:H and SiO_x/SiN_x:H layers attract electrons due to positive layer charge as discussed before, AlO_x:H/SiN_x:H samples feature a high concentration of holes close to the surface due to negative charge of the AlO_x:H layer. Likewise, other charged particles, such as hydrogen ions, could accumulate or move away from the surface depending on the sign of fixed charge in the dielectric layers.

A closer investigation of SiN_x:H passivated FZ-Si samples revealed that chemical passivation quality decreases significantly for treatment times >10 h at 80 °C and ∼1 sun equivalent illumination whereas the fixed charge density remains rather unchanged (see Fig. 2 and [15]). In all investigated samples, similar types of bonds exist at the silicon surface such as Si–O, Si–Si, or Si–H bonds. Therefore, the interface defect density D_{it} could be affected in a similar manner in the differently coated samples in a region close to the interface, e.g., by generation of new dangling bonds.

One possible degradation mechanism might be found in the evolution of hydrogen bonding states. All of the investigated layers feature a hydrogen-rich SiN_x:H layer and received a firing step. It is commonly assumed that the improvement of passivation quality during a firing step is, at least in part, re-

lated to a hydrogen passivation of interface states [32], [33]. Accordingly, a loss of hydrogen at higher annealing temperatures as suggested in [34]–[36] or a reconfiguration of hydrogen bonding states [37], [38] could lead to a decrease in surface passivation quality. Such a hydrogen-based degradation mechanism could also explain why a nonfired sample and an annealed sample show significantly less degradation of surface passivation quality compared to a fired sample as described in [14]. Additionally, hydrogen could be trapped at boron atoms, explaining why material with higher boron doping suffers from a faster or stronger degradation of surface passivation quality. However, if hydrogen loss is causing the degradation, the observed recovery of passivation quality at higher treatment temperatures would then have to be explained without hydrogen and might be related to a rearrangement of (dangling) bonds. The mechanism could also involve the stepwise evolution of hydrogen containing defects (e.g., hydrogen platelets [39], [40]) which may have formed during cool-down of the deposition or firing step in a region close to the surface. In general, further research has to be conducted to clarify whether hydrogen actually is involved in the degradation of surface passivation as observed in this study.

Already now it can be stated that degradation of surface passivation quality may significantly influence the outcome and interpretation of LID studies aimed at the investigation of bulk defects. This has been demonstrated on a regenerated Cz-Si and a nonregenerated mc-Si sample: After long treatment times, the surface passivation limits τ_{eff} in both samples, making it hard to draw conclusions about the long-term evolution of τ_b. Therefore, it is strongly advised to check for changes in surface passivation quality when performing LID experiments, e.g., by tracking J_{0s} values. In general, AlO_x:H/SiN_x:H appears to be the best choice for long-term experiments on lifetime samples when a stable passivation quality is required.

Since SiO_x/SiN_x:H and AlO_x:H/SiN_x:H passivation layers are used for rear side passivation of PERC solar cells, too, a similar degradation might occur on cell level as well. AlO_x:H/SiN_x:H passivated samples treated at 60 °C and 0.1 equivalent suns (and therefore in a similar temperature and injection range compared to PERC cells) show the onset of surface-related degradation after $>$1000 h of treatment (data not shown). However, the investigated lifetime samples were neither separated from ambient air nor metalized, and it is unclear yet whether a similar degradation might affect the rear side passivation of real PERC solar cells, too.

V. Conclusion

Lifetime samples are often passivated with pure SiN_x:H layers. It was observed that this passivation method can be prone to a severe degradation of surface passivation quality during LID treatments, followed by a recovery of surface passivation quality observable at higher treatment temperatures. It was shown that a time-resolved calculation of J_{0s} is a useful tool to assess the degree of degradation in surface passivation quality, even when changes in τ_b occur simultaneously. The observed degradation can significantly influence the outcome and interpretation of measurement data from LID experiments both in mc-Si as well as in Cz-Si as was discussed in detail.

This surface-related degradation is not simply avoidable by using other passivation layers: SiO_x/SiN_x:H and AlO_x:H/SiN_x:H passivated and fired samples may also show a significant degradation and subsequent recovery of surface passivation quality during LID treatments. As these layer stacks are applied for rear surface passivation of PERC cells, it can be suspected that a similar degradation may occur on cell level, too, and thus solar cell efficiency could suffer in the long term even under field conditions. However, the degradation proceeds much slower in AlO_x:H/SiN_x:H passivated samples, making this layer stack comparably long-term stable.

Acknowledgment

The authors would like to thank A. Zuschlag from the University of Konstanz and N. Grant as well as J. Murphy from the University of Warwick for wet chemical repassivation of samples using superacids. Also acknowledged are A. Heilemann, L. Mahlstaedt, J. Rinder, F. Mutter, B. Rettenmaier, J. Engelhardt, and S. Joos from the University of Konstanz for technical support. The content is the responsibility of the authors.

References

[1] J. Lindroos and H. Savin, "Review of light-induced degradation in crystalline silicon solar cells," *Sol. Energy Mater. Sol. Cells*, vol. 147, pp. 115–126, 2016.

[2] H. Fischer and W. Pschunder, "Investigation of photon and thermal induced changes in silicon solar cells," in *Proc. 10th IEEE Photovolt. Spec. Conf. Rec.*, Palo Alto, CA, USA, 1974, pp. 404–411.

[3] K. Bothe and J. Schmidt, "Electronically activated boron-oxygen-related recombination centers in crystalline silicon," *J. Appl. Phys.*, vol. 99, 2006, Art. no. 013701.

[4] T. Niewelt, J. Schön, W. Warta, S. W. Glunz, and M. C. Schubert, "Degradation of crystalline silicon due to boron–oxygen defects," *IEEE J. Photovolt.*, vol. 7, no. 1, pp. 383–398, Jan. 2017.

[5] K. Ramspeck *et al.*, "Light induced degradation of rear passivated mc-Si solar cells," in *Proc. 27th Eur. Photovolt. Sol. Energy Conf. Exhib.*, Frankfurt, Germany, 2012, pp. 861–865.

[6] F. Fertig, K. Krauß, and S. Rein, "Light-induced degradation of PECVD aluminium oxide passivated silicon solar cells," *Phys. Status Solidi RRL*, vol. 9, pp. 41–46, 2015.

[7] F. Kersten *et al.*, "Degradation of multicrystalline silicon solar cells and modules after illumination at elevated temperature," *Sol. Energy Mater. Sol. Cells*, vol. 142, pp. 83–86, 2015.

[8] A. W. Blakers, A. Wang, A. M. Milne, J. Zhao, and M. A. Green, "22.8% efficient silicon solar cell," *Appl. Phys. Lett.*, vol. 55, pp. 1363–1365, 1989.

[9] A. Herguth, G. Schubert, M. Kaes, and G. Hahn, "A new approach to prevent the negative impact of the metastable defect in boron doped Cz silicon solar cells," in *Proc. 3rd World Conf. Photovolt. Energy Convers.*, Waikoloa, HI, USA, 2006, pp. 940–943.

[10] A. Herguth, G. Schubert, M. Kaes, and G. Hahn, "Investigations on the long time behavior of the metastable boron-oxygen complex in crystalline silicon," *Prog. Photovolt.*, vol. 16, pp. 135–140, 2008.

[11] F. Kersten *et al.*, "Degradation of multicrystalline silicon solar cells and modules after illumination at elevated temperature," *Sol. Energy Mater. Sol. Cells*, vol. 142, pp. 83–86, 2015.

[12] A. Zuschlag, D. Skorka, and G. Hahn, "Degradation and regeneration in mc-Si after different gettering steps," *Prog. Photovolt.*, vol. 25, pp. 545–552, 2017.

[13] D. Sperber, A. Herguth, and G. Hahn, "Instability of dielectric surface passivation quality at elevated temperature and illumination," *Energy Procedia*, vol. 92, pp. 211–217, 2016.

[14] D. Sperber, F. Furtwängler, A. Herguth, and G. Hahn, "On the stability of dielectric passivation layers under illumination and temperature treatment," in *Proc. 32nd Eur. Photovolt. Sol. Energy Conf. Exhib.*, Munich, Germany, 2016, pp. 523–526.

[15] D. Sperber, A. Heilemann, A. Herguth, and G. Hahn, "Temperature and light induced changes in bulk and passivation quality of boron-doped float-zone silicon coated with SiN_x:H," *IEEE J. Photovolt.*, vol. 7, no. 2, pp. 463–470, Mar. 2017.

[16] K. R. McIntosh and L. E. Black, "On effective surface recombination parameters," *J. Appl. Phys.*, vol. 116, 2014, Art. no. 014503.

[17] A. Herguth, "On the meaning(fullness) of the intensity unit 'suns' in light induced degradation experiments," *Energy Procedia*, vol. 124, pp. 53–59, 2017.
[18] A. Kimmerle, J. Greulich, and A. Wolf, "Carrier-diffusion corrected J_0-analysis of charge carrier lifetime measurements for increased consistency," *Sol. Energy Mater Sol. Cells*, vol. 142, pp. 116–122, 2015.
[19] A. L. Blum, J. S. Swirhun, R. A. Sinton, and A. Kimmerle, "An updated analysis to the WCT-120 QSSPC measurement system using advanced device physics," in *Proc. 28th Eur. Photovolt. Sol. Energy Conf. Exhib.*, Paris, France, 2013, pp. 1521–1523.
[20] A. Kimmerle, P. Rothhardt, A. Wolf, and R. A. Sinton, "Increased reliability for J_0-analysis by QSSPC," *Energy Procedia*, vol. 55, pp. 101–106, 2014.
[21] W. Shockley and W. T. Read Jr., "Statistics of the recombinations of holes and electrons," *Phys. Rev.*, vol. 87, pp. 835–842, 1952.
[22] R. N. Hall, "Electron-hole recombination in germanium," *Phys. Rev.*, vol. 87, p. 387, 1952.
[23] D. Kiliani *et al.*, "Minority charge carrier lifetime mapping of crystalline silicon wafers by time-resolved photoluminescence imaging," *J. Appl. Phys.*, vol. 110, 2011, Art. no. 054508.
[24] D. Kiliani, A. Herguth, G. Micard, J. Ebser, and G. Hahn, "Time-resolved photoluminescence imaging with electronic shuttering using an image intensifier unit," *Sol. Energy Mater. Sol. Cells*, vol. 106, pp. 55–59, 2012.
[25] J. Bullock *et al.*, "Superacid passivation of crystalline silicon surfaces," *ACS Appl. Mater. Interfaces*, vol. 8, pp. 24205–24211, 2016.
[26] N. E. Grant *et al.*, "Superacid-treated silicon surfaces: Extending the limit of carrier lifetime for photovoltaic applications," *IEEE J. Photovolt.*, to be published. Doi: 10.1109/JPHOTOV.2017.2751511.
[27] D. Sperber, A. Graf, A. Heilemann, A. Herguth, and G. Hahn, "Bulk and surface instabilities in boron doped float-zone samples during light induced degradation treatments," *Energy Procedia*, vol. 124, pp. 794–798, 2017.
[28] D. Sperber, A. Herguth, and G. Hahn, "A 3-state defect model for light induced degradation in boron-doped float-zone silicon," *Phys. Status Solidi RRL*, vol. 11, 2017, Art. No. 1600408.
[29] D. Macdonald, J. Tan, and T. Trupke, "Imaging interstitial iron concentrations in boron-doped crystalline silicon using photoluminescence," *J. Appl. Phys.*, vol. 103, 2008, Art. no. 073710.
[30] H. Haug and J. Greulich, "PC1Dmod 6.2 – Improved simulation of c-Si devices with updates on device physics and user interface," *Energy Procedia*, vol. 92, pp. 60–68, 2016.
[31] T. Niewelt, W. Kwapil, M. Selinger, A. Richter, and M. C. Schubert, "Long-term stability of aluminium oxide based surface passivation schemes under illumination at elevated temperatures," *IEEE J. Photovolt.*, vol. 7, no. 5, pp. 1197–1202, Sep. 2017.
[32] J.-F. Lelièvre *et al.*, "Study of the composition of hydrogenated silicon nitride SiN_x:H for efficient surface and bulk passivation of silicon," *Sol. Energy Mater. Sol. Cells*, vol. 93, pp. 1281–1289, 2009.
[33] G. Dingemans, W. Beyer, M. C. M. van de Sanden, and W. M. M. Kessels, "Hydrogen induced passivation of Si interfaces by Al_2O_3 films and SiO_2/Al_2O_3 stacks," *Appl. Phys. Lett.*, vol. 97, 2010, Art. no. 152106.
[34] T. C. Kho, K. R. McIntosh, J. T. Tan, A. F. Thomson, and F. W Chen, "Removal of hydrogen and deposition of surface charge during rapid thermal annealing," in *Proc. 33rd IEEE Photovolt. Spec. Conf. Rec.*, San Diego, CA, USA, 2008, pp. 1–5.
[35] T. C. Kho, L. E. Black, and K. R. McIntosh, "Degradation of Si–SiO_2 interfaces during rapid thermal annealing," in *Proc. 24th Eur. Photovolt. Sol. Energy Conf. Exhib.*, Hamburg, Germany, 2009, pp. 1586–1590.
[36] F. W. Chen, J. E. Cotter, A. Cuevas, S. Winderbaum, and K. Roth, "Anomalous thermal behaviour of surface passivation by PECVD silicon nitride on p-type crystalline silicon," in *Proc. 20th Eur. Photovolt. Sol. Energy Conf. Exhib.*, Barcelona, Spain, 2005, pp. 1419–1422.
[37] S. McQuaid, M. J. Binns, R. C. Newman, E. C. Lightowlers, and J. B. Clegg, "Solubility of hydrogen in silicon at 1300 °C," *Appl. Phys. Lett.*, vol. 62, pp. 1612–1614, 1993.
[38] R. Jones, B. J. Coomer, J. P. Goss, B. Hourahine, and A. Resende, "The interaction of hydrogen with deep level defects in silicon," *Solid State Phenom.*, vol. 71, pp. 173–248, 2000.
[39] N. M. Johnson, F. A. Ponce, R. A. Street, and R. J. Nemanich, "Defects in single-crystal silicon induced by hydrogenation," *Phys. Rev. B*, vol. 35, pp. 4166–4169, 1987.
[40] S. B. Zhang and W. B. Jackson, "Formation of extended hydrogen complexes in silicon," *Phys. Rev. B*, vol. 43, pp. 12142–12145, 1991.